JOURNAL OF VIROLOGY, Jan. 1997, p. 495–500 Vol. 71, No. 1
0022-538X/97/$04.00+0

Magnesium-Induced Conformational Change of Packaging RNA for Procapsid Recognition and Binding during Phage ϕ29 DNA Encapsidation

CHAOPING CHEN AND PEIXUAN GUO*

Department of Pathobiology and Purdue Biochemistry & Molecular Biology Program, Purdue University, West Lafayette, Indiana 47907

Received 19 June 1996/Accepted 17 September 1996

Bacteriophage ϕ29 is typical of double-stranded DNA viruses in that its genome is packaged into a preformed procapsid during maturation. An intriguing feature of ϕ29 assembly is that a virus-encoded RNA (pRNA) is required for the packaging of its genomic DNA. Psoralen cross-linking, primer extension, and T_1 RNase partial digestion revealed that pRNA had at least two conformations; one was able to bind procapsids, and the other was not. In the presence of Mg^{2+}, one stretch of pRNA, consisting of bases 31 to 35, was confirmed to be proximal to base 69, as revealed by its efficient cross-linking by psoralen. Two cross-linking sites in the helical region were identified. Mg^{2+} induced a conformational change of pRNA that exposes the portal protein binding site by promoting the refolding of two strands of the procapsid binding region, resulting in the formation of pRNA-procapsid complexes. The procapsid binding region in this binding-competent conformation could not be cross-linked with psoralen. When the two strands of the procapsid binding region were fastened by cross-linking, pRNA could neither bind procapsids nor package ϕ29 DNA. A pRNA conformational change was also discernible by comparison of migration rates in native EDTA and Mg^{2+} polyacrylamide gel electrophoresis and was revealed by T_1 RNase probing. The Mg^{2+} concentration required for the detection of a change in pRNA cross-linking patterns was 1 mM, which was the same as that required for pRNA-procapsid complex formation and DNA packaging and was also close to that in normal host cells.

Bacteriophage ϕ29 of *Bacillus subtilis* packages its genomic DNA into a procapsid with the aid of the DNA-packaging ATPase gp16 during its maturation. We have been able to package ϕ29 DNA into procapsids in a defined in vitro system with up to 90% efficiency (8, 10, 11). The DNA-filled procapsids can be converted to infectious virions after the in vitro addition of neck, tail, and morphogenic proteins produced from cloned genes (17, 18), thereby providing a convenient assay for the function of packaging components (7, 11, 19, 24, 25, 32, 34, 35). One intriguing feature of ϕ29 is that a 120-base ϕ29-encoded RNA (pRNA) is required for DNA encapsidation (6). The presence of similar RNA molecules has been identified in the *B. subtilis* double-stranded DNA phages SF5, M2, NF, GA1, and PZA (1), as well as in phage Cp-1 of *Streptococcus pneumoniae* (20). Phylogenetic analysis of all reported pRNAs from both *B. subtilis* and *S. pneumoniae* phages shows very low sequence homology and few conserved bases, yet members of the family of pRNAs appear to have similar predicted secondary structures (1, 20). Beyond its presence in phages, there is only postulation of such RNA involvement in genome encapsidation of other animal viruses, such as poxvirus (21) or adenovirus (14). Nonetheless, the requirement for pRNA is very specific (1, 11, 34), since pRNAs from these related viruses fail to function in ϕ29 DNA packaging (1), as do RNA pools from *Escherichia coli*, including 5S rRNA (11). Also, single-base mutations can result in the loss of pRNA activity (22, 23, 25, 28, 29, 32, 34). Each procapsid possesses six copies of pRNA molecules, and all of them are needed for the translocation of ϕ29 genomic DNA (22, 24, 25, 28). pRNA can be a potential target for antiviral agents. We have demonstrated strong inhibition of viral assembly by targeting pRNA with antisense oligonucleotides in vitro (33) and complete blockage of plaque formation with mutant pRNA in vivo (25).

RNA molecules are able to play both structural and enzymatic roles. Understanding of RNA structure will facilitate the elucidation of RNA function. ϕ29 pRNA has been found to play a vital role in the DNA translocation process, which involves energy transformation. How could pRNA perform a physical task in collaborating with other components to force the DNA into the protein shell? Obviously, the conformational change of pRNA is one of the aspects involved in explication of a process involving migration and motion. More than one conformational change in pRNA is expected during this elaborate and intricate DNA packaging process. The interaction of pRNA with each participating component, such as Mg^{2+}, ATP, DNA packaging protein gp16, DNA-gp3, and procapsids, might result in respective conformational changes. Although RNA conformational change could be a universal process, information regarding this process is limited.

Mg^{2+} is required for the packaging of ϕ29 DNA (3, 9). In the presence of Mg^{2+}, pRNA is known to bind to the portal vertex (5, 22), an oligomeric aperture through which DNA passes to enter the capsid (26). Many interesting questions about pRNA remain to be answered. For example, what is the actual role of Mg^{2+}? How does Mg^{2+} cause a pRNA-procapsid interaction? Does Mg^{2+} bind to the portal vertex and cause a conformational change of the portal vertex that results in the recruitment of pRNA, or does Mg^{2+} interact with pRNA and cause a pRNA conformational change that results in its binding to the procapsid? Does Mg^{2+} simply serve as a bridge for a pRNA-portal vertex linkage? The answers to these questions might help in the elucidation of the biochemical role of pRNA. In this paper, we report that Mg^{2+} induced a conformational

* Corresponding author. Mailing address: B-36 Hansen Life Sciences Research Building, Cancer Research Center, Purdue University, West Lafayette, IN 47907. Phone: (317) 494-7561. Fax: (317) 496-1795. E-mail: guo@vet.purdue.edu.

change in pRNA, which led to the subsequent binding of pRNA to the portal vertex.

MATERIALS AND METHODS

Synthesis of pRNA molecules. Plasmid PCR7/11, a derivative of PCRII (Invitrogen, San Diego, Calif.) containing coding sequences of wild-type-phenotype pRNA 7/11 (35), was linearized with *Eco*RI. The resulting linearized DNA served as a template to generate RNA fragments by in vitro transcription with T7 RNA polymerase as described previously (32, 35).

Electrophoretic mobility assays. pRNA (0.1 to 0.2 μg) was applied onto an 8% nondenaturing polyacrylamide gel (monomer/bis ratio, 19:1) with TBM (89 mM Tris-borate [pH 8.0], 1 mM $MgCl_2$) (31) or TBE (89 mM Tris-borate, 2 mM EDTA, pH 8.0) as the running buffer. The relative mobility of pRNA was compared with those of nonspecific RNA and a DNA ladder.

Psoralen cross-linking. Cross-linking of pRNA with 4′-aminomethyl-4,5′,8-trimethylpsoralen (AMT) was performed as described previously (27). Briefly, 0.2 to 1.0 μg of pRNA in 10 μl of H_2O, unless otherwise indicated, and 1 μl of 200-ng/ml AMT were mixed on ice and then spotted onto prechilled Parafilm floating on ice water, with each drop less than 10 μl. The samples were irradiated with long-wave UV from a UVGL-25 instrument (UVP Inc.) with a distance of 4 to 5 cm for 50 to 60 min. The cross-linked mixture was mixed with an equal volume of 2× loading buffer (0.01% xylene, 0.01% bromophenol blue, 10 M urea in 0.1× TBE) before being loaded onto an 8 M urea–10% polyacrylamide gel to separate cross-linked products from un-cross-linked pRNA. Both the cross-linked and un-cross-linked pRNAs were excised from the gel, eluted, and ethanol precipitated for further analysis.

Primer extension. The modified avian myeloblastosis virus (AMV) reverse transcriptase primer extension system (Promega) was used. One microliter (100 fmol) of ^{32}P-labeled primer and 50 to 100 ng of pRNA in 5 μl of H_2O were mixed with 5 μl of 2× AMV PE (primer extension) buffer and then heated at 65°C for 20 min. The reaction mixtures were then cooled at room temperature for 10 min to anneal the primer and RNA. Elongation was initiated by adding 5 μl of 2× AMV PE buffer, 2 μl of 40 mM sodium pyrophosphate, 1 μl of AMV reverse transcriptase (1 U/μl), and 1 μl of nuclease-free H_2O. The reaction mixture was incubated at 54°C for 30 min. Each sample was then mixed with 20 μl of loading buffer and heated to 90°C for 10 min, and 8 μl of each sample was loaded directly onto an 8% sequencing gel.

T_1 RNase probing. Ten to 20 nanograms of 5′-end ^{32}P-labeled pRNA (approximately 3,000 cpm) in 2 μl of H_2O was mixed with 6 μl of carrier tRNA (1.75 μg/μl) and dialyzed on a 0.025-μm-pore-size type VS filter membrane (Millipore Corp.) against TBE for 15 min. Half of the sample was then transferred into an Eppendorf tube, and the other half was further dialyzed on the VS filter membrane against TMS (50 mM Tris [pH 7.8], 100 mM NaCl, 10 mM $MgCl_2$) for 30 min. One microliter of T_1 RNase (1 U/μl; from the RNA-sequencing kit from U.S. Biochemicals) was added to both samples. After 15 min at ambient temperature, the reactions were stopped by adding an equal volume of stop solution (95% formamide, 0.025% xylene, 10 mM EDTA), and the mixtures were loaded onto an 8% sequencing gel. Both T_1 RNase and alkaline hydrolysis ladders were generated according to the instructions in the RNA-sequencing kit (U.S. Biochemicals).

Assays for pRNA binding to procapsids. Binding assays were performed by using sucrose gradient sedimentation to determine an Mg^{2+} requirement for procapsid binding (5). Briefly, 10 μl of purified procapsids (2 mg/ml) was dialyzed on a 0.025-μm-pore-size type VS filter membrane (Millipore Corp.) against TBE buffer (17) for 10 min at ambient temperature to remove residual Mg^{2+}, and then [^{3}H]pRNA was added. After being dialyzed for another 15 min against TBE, the mixtures were dialyzed against TS buffer (50 mM Tris [pH 7.8], 100 mM NaCl), with various concentrations of $MgCl_2$, for 30 min at ambient temperature. After incubation, the mixtures were diluted with 0.1 ml of TS containing the respective concentration of $MgCl_2$ and then loaded on top of a 5 to 20% sucrose gradient (prepared in TS containing the respective concentration of $MgCl_2$) and spun in a Beckman L-80 ultracentrifuge at 35,000 rpm for 30 min at 20°C in a SW55 rotor. Fractions were collected from the bottom of the tube and subjected to liquid scintillation counting.

In vitro ϕ29 assembly. The purification of procapsids (7, 11, 12), gp16 (8), and DNA-gp3 (17); the preparation of neck and tail extracts (17–19); and the assembly of infectious ϕ29 virion in vitro (17–19) have been described previously. Briefly, purified procapsids (2 mg/ml) were dialyzed on a 0.025-μm-pore-size type VS filter membrane (Millipore Corp.) against TBE for 10 min at room temperature. Mixtures of mutant and wild-type pRNAs (in nuclease-free H_2O) in various ratios were added to the dialyzed procapsids. The procapsid-pRNA mixtures were dialyzed for another 15 min against TBE and then for 30 min against TMS. The pRNA-enriched procapsids were mixed with gp16, DNA-gp3, and reaction buffer (10 mM ATP, 6 mM 2-mercaptoethanol, and 3 mM spermidine in TMS) to complete the DNA-packaging reaction. After 30 min, neck, tail, and morphogenic proteins were added to the DNA-packaging reaction mixtures to complete the assembly of infectious virions, which were assayed by standard plaque formation.

RESULTS

Mg^{2+} caused a pRNA conformational change revealed by native PAGE. The effect of Mg^{2+} on pRNA conformation was investigated with native 8% polyacrylamide gel electrophoresis (PAGE) (Fig. 1). In the absence of Mg^{2+} and the presence of EDTA, pRNA migrated in the gel with a rate similar to that of a DNA fragment of 105 bp (Fig. 1A, lane b). In the presence of 1 mM Mg^{2+} and the absence of EDTA, however, pRNA migrated faster, with a rate similar to that of a 120-base control RNA and a DNA fragment of 78 bp (Fig. 1B, lane b), indicating that only 1 mM Mg^{2+} was sufficient to induce a pRNA conformational change. The migration rates of the 120-base control 5S rRNA were very similar in EDTA and Mg^{2+} gels, indicating that its migration rate was not affected by Mg^{2+} (Fig. 1, lanes a) and suggesting that the effect of Mg^{2+} was specific to pRNA in this case. Furthermore, to exclude any contamination and degradation, the pRNA band was excised and eluted and was used to package genome DNA by using an in vitro assembly system. It functioned as efficiently as the positive control.

T_1 RNase probing verified a conformational change of pRNA. The Mg^{2+}-induced pRNA conformational change was verified by T_1 RNase probing (Fig. 2). The pattern of partial digestion of pRNA by T_1 provided strong evidence for the presence of two conformations, dependent on the presence or absence of Mg^{2+}. Without Mg^{2+}, strong cleavages by T_1 were seen at pRNA G_{28}, G_{30}, and G_{34} (Fig. 2, lane B), while with Mg^{2+}, these three G's became more resistant to T_1 attack (Fig. 2, lane D), indicating a conformation change or refolding of pRNA caused by Mg^{2+}.

Conformational change of pRNA induced by Mg^{2+} analyzed by psoralen cross-linking. The effect of Mg^{2+} on a pRNA conformational change was further investigated by psoralen cross-linking and electrophoresis in 8 M urea–8% polyacrylamide gels (Fig. 3). Without Mg^{2+}, about 40 to 70% of pRNA was cross-linked and migrated slower in urea denaturing gels (Fig. 3, lane b). When 1 mM Mg^{2+} was present, the cross-linked band was almost undetectable in the gel (Fig. 3, lane c). When the concentration of Mg^{2+} was increased to 5 mM, no such detectable cross-linked pRNAs were observed (Fig. 3, lane d). It has been reported that the cross-linking efficiency of RNA with psoralen is not affected by Mg^{2+} (27). Control experiments with *E. coli* 5S rRNA (Fig. 3, lanes h and l) showed that Mg^{2+} did not affect the cross-linking of 5S rRNA by psoralen (Fig. 3, lanes h to m). The data suggested that the Mg^{2+} effects on the cross-linking pattern were specific to pRNA. Furthermore, the Mg^{2+}-induced conformational change was reversible, since the addition of 10 mM EDTA after incubation of pRNA with 5 mM Mg^{2+} resulted in the reappearance of the cross-linked pRNA band (Fig. 3, lane e).

To exclude the possibility that the inhibition of cross-linking was due to the competition of positively charged Mg^{2+} with psoralen for interaction with the negatively charged RNA, 5 mM Na^+ was substituted for Mg^{2+} in cross-linking reactions. Cross-linking was not inhibited when Mg^{2+} was replaced with Na^+ (Fig. 3, lanes f and g). Similarly, pRNA was mixed with psoralen first and incubated on ice for 10 min before the addition of 5 mM Mg^{2+}. No detectable cross-linked bands were observed (data not shown), suggesting that Mg^{2+}-induced inhibition of psoralen cross-linking was not caused by the competition of positively charged Mg^{2+} with psoralen for sites of interaction with pRNA. The inhibition of cross-linking of pRNA was also observed with other divalent metal ions, such as Mn^{2+}, Ca^{2+}, Co^{2+}, Cd^{2+}, and Zn^{2+} at concentrations of 5 mM (data not shown).

Identification of cross-linking sites. Psoralen has been used as a photoactive probe for nucleic acid structures (4, 15, 27, 30). Psoralen intercalates into RNA molecules, and upon irradiation with 320- to 400-nm light, it freezes proximal uridines of RNA that are within a certain distance and in certain stereo positions (helix, pseudoknot, etc.) by covalent attachment. The preferred nucleotides for intercalation are pyrimidines (U > C > A > G). Primer extension was used to identify the sites of cross-linking with primers to variable locations. Cross-linking sites in cross-linked pRNAs obtained without Mg^{2+} were shown (Fig. 4 and 5). All sites were located in one predicted helical region in the middle of the pRNA (Fig. 5A). In the upper strand there was a strong stop at U_{36} and two weak stops at G_{34} and A_{32}, which indicate a strong cross-linking site at U_{35} and two weak cross-linking sites at U_{31} and U_{33}, since primer extension stops one base prior to the cross-linked site (13). In the lower strand there was a strong stop at A_{70} and a weak stop at A_{68}, which indicate a strong cross-linking site at U_{69} and a weak cross-linking site at C_{67}.

The two strong stop sites were U_{35} and U_{69}. Both U's are located in a predicted helical region. However, no cross-linking occurred at these two locations when Mg^{2+} was present, indicating that Mg^{2+} caused refolding of pRNA. Also, this cross-linked region has been found to contact portal protein directly (Fig. 5) (22, 33). Refolding of the helix might provide a suitable structure for the binding to portal protein gp10. It is interesting to find that the strongest cross-linking site in the upper strand was neither U_{31} nor U_{33}, as expected from computer predictions, but U_{35}. The detailed tertiary structure of this helical region remains to be further investigated.

When excess psoralen is used in RNA cross-linking, monoadducts (one psoralen molecule attaches to one U only) will be the major side products. In our case, pRNAs with monoadducts had a migration rate similar to that of un-cross-linked normal pRNA in the urea gel. These pRNAs were active in ϕ29 assembly, although with a 10-fold decrease in activity. The pRNAs with monoadducts showed extra stops in primer extension (Fig. 4A, lane e) in comparison to wild-type-phenotype pRNA (Fig. 4A, lane b).

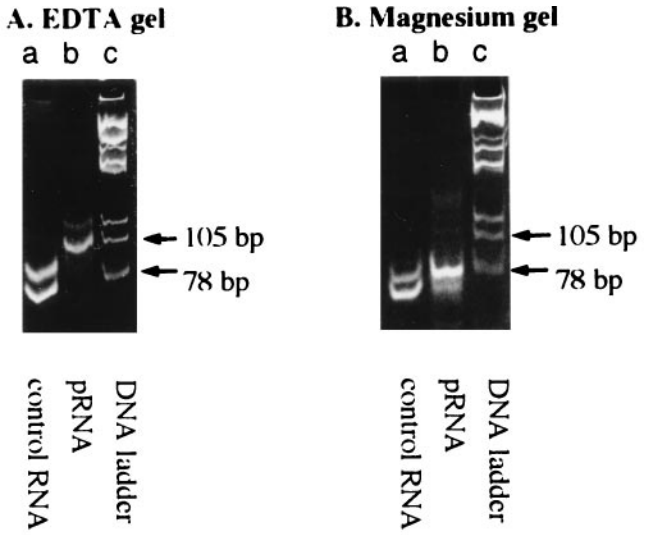

FIG. 1. Native 8% PAGE demonstrating the change of the migration rate of pRNA in the absence (A) and presence (B) of Mg^{2+}. pRNA or a 120-base control RNA was incubated with (B) and without (A) 1 mM Mg^{2+} and subjected to Mg^{2+} (B) and EDTA (A) gel electrophoresis. Lanes a, b, and c, 120-base control 5S rRNA, pRNA, and DNA ladder, respectively.

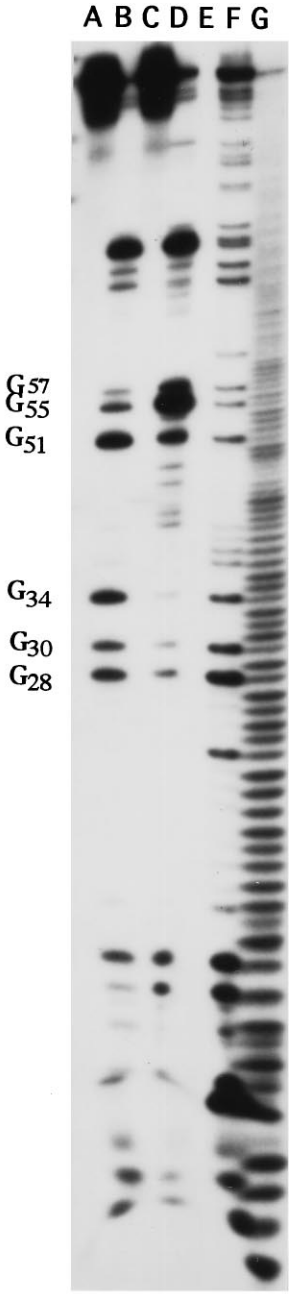

FIG. 2. T_1 RNase digestion of pRNA with and without Mg^{2+} treatment. Lane A, pRNA without Mg^{2+} and T_1; lane B, T_1 digestion of pRNA without Mg^{2+}; lane C, pRNA with Mg^{2+} and without T_1 digestion; lane D, T_1 digestion of pRNA with Mg^{2+}; lane E, blank; lane F, T_1 digestion of pRNA under denaturing conditions; lane G, alkaline-hydrolyzed pRNA.

Minimum Mg^{2+} concentration requirement. To understand the role of Mg^{2+}, the minimum Mg^{2+} concentration requirement for pRNA binding to procapsids was further analyzed with the use of sucrose gradient sedimentation (Fig. 6). One millimolar was required and sufficient for the binding of pRNA to procapsids. The same threshold concentration of 1 mM was observed for the packaging of ϕ29 DNA and for the assembly of infectious ϕ29 particles (data not shown). Since a prerequisite for the assembly of infectious virions is the packaging of ϕ29 DNA and since a prerequisite for DNA packaging is the

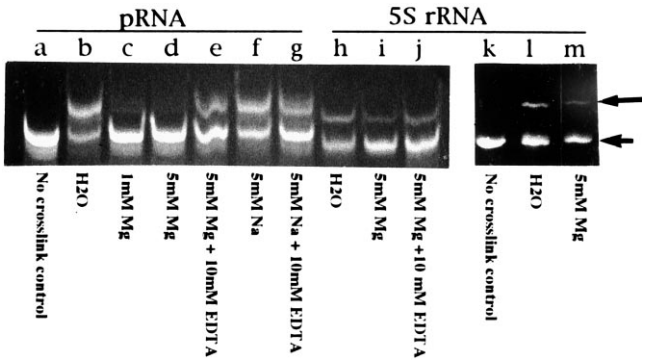

FIG. 3. Denaturing polyacrylamide gel showing a change of pRNA migration rate caused by cross-linking. Cross-linking of pRNA and control 5S rRNA was examined by 8 M urea–PAGE with 8% (lanes a to j) and 10% (lanes k to m) polyacrylamide. The band with a lower migration rate was a result of psoralen cross-linking. Lane a, pRNA control without cross-linking; lane b, cross-linking of pRNA alone; lane c, cross-linking of pRNA in the presence of 1 mM Mg; lane d, cross-linking of pRNA in the presence of 5 mM Mg^{2+}; lane e, cross-linking of pRNA in the presence of 5 mM Mg and 10 mM EDTA; lane f, cross-linking of pRNA in the presence of 5 mM Na^{+}; lane g, cross-linking of pRNA in the presence of 5 mM Na^{+} and 10 mM EDTA; lanes h and l, cross-linking of 5S rRNA alone; lanes i and m, cross-linking of 5S rRNA in the presence of 5 mM Mg^{2+}; lane j, cross-linking of 5S rRNA in the presence of 5 mM Mg^{2+} and 10 mM EDTA; lane k, 5S rRNA control without cross-linking.

binding of pRNA to procapsids, the identical requirement of 1 mM Mg^{2+} in both of these reactions suggests that the requirement of Mg^{2+} might be related to the first step of the reaction, i.e., the conformational change of pRNA before binding to procapsids.

It has been reported that Mg^{2+} frequently promotes reactions in which RNA is involved, such as protein recognition or RNA-protein interaction (16). Stabilization of the RNA structure by Mg^{2+} has been categorized into two classes with respect to Mg^{2+} binding sites. Class 2 interactions are nonspecific, predominantly electrostatic interactions between the ion and the RNA backbone phosphates. For this class, the Mg^{2+} concentration needed is generally more than 0.1 M. Class 1 interactions are generally more specific with a higher affinity (K_D of around 0.1 to 1 mM). A Mg^{2+} requirement of 1 mM in pRNA-procapsid binding is within the range of those previously reported for class 1 interactions. Whether there is a specific Mg^{2+} binding site within pRNA remains to be investigated. The 1 mM concentration reported here is the threshold concentration rather than the optimal concentration reported by Reid et al. (22).

Cross-linked pRNA is incompetent for procapsid binding and DNA packaging. To further test whether the refolding of the two strands in a procapsid binding region is needed for pRNA to bind procapsids and to package ϕ29 DNA, active pRNA was cross-linked with psoralen. After cross-linking, pRNAs with different conformations were separated by denaturing PAGE. The band corresponding to the cross-linked pRNA was isolated from the gel and purified. Primer extension was performed to verify the cross-linking sites. Our results showed that the cross-linked pRNA was not able to bind procapsids, nor was it active in ϕ29 DNA packaging (Fig. 7). The un-cross-linked pRNA band was also isolated. This un-cross-linked pRNA was able to package ϕ29 DNA (data not shown) with less than a 10-fold reduction, indicating the incompetence of the cross-linked pRNA in ϕ29 procapsid binding and indicating that DNA packaging was not due to the influence of psoralen monoadducts resulting from UV irradiation. These results indicate that refolding of the helix consisting of box A and/or box B (Fig. 5B), within the procapsid binding region, is required for the binding of pRNA to procapsids.

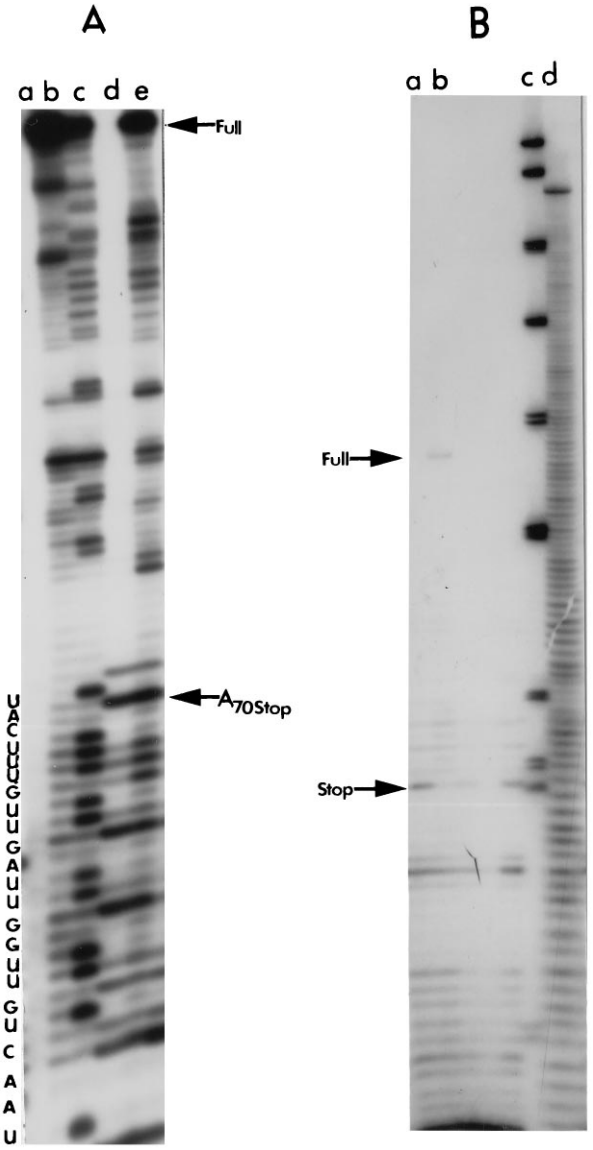

FIG. 4. Primer extension to detect the cross-linking sites. Each lane contained all components for an extension reaction except as noted. Full, expected full-length DNA by extension to the 5′ end of pRNA; Stop, location of an extension termination due to a cross-link. (A) Extension with primer P11. Lane a, mock (without pRNA); lane b, un-cross-linked pRNA without psoralen treatment; lane c, same as lane b except with the addition of ddATP to mark the location of U stops; lane d, cross-linked pRNA leading to a strong stop at A_{70} and a weak stop at A_{68}; lane e, un-cross-linked pRNA band isolated from psoralen-treated and cross-linked samples directed the synthesis of a full-length DNA. (B) Extension with primer P19. Lane a, cross-linked pRNA, leading to a strong stop at U_{36} and two weak stops at G_{34} and A_{32}; lane b, un-cross-linked pRNA band isolated from psoralen-treated and cross-linked samples directed the synthesis of a full-length DNA; lane c, ϕX174-*Hin*fI DNA marker; lane d, NaOH-hydrolyzed pRNA ladder.

DISCUSSION

We found that Mg^{2+} is required for the binding of pRNA to procapsids (5). Without Mg^{2+}, two stretches of pRNA sequences, referred to as box A and box B (Fig. 5B), were efficiently cross-linked by psoralen, suggesting that, in the ab-

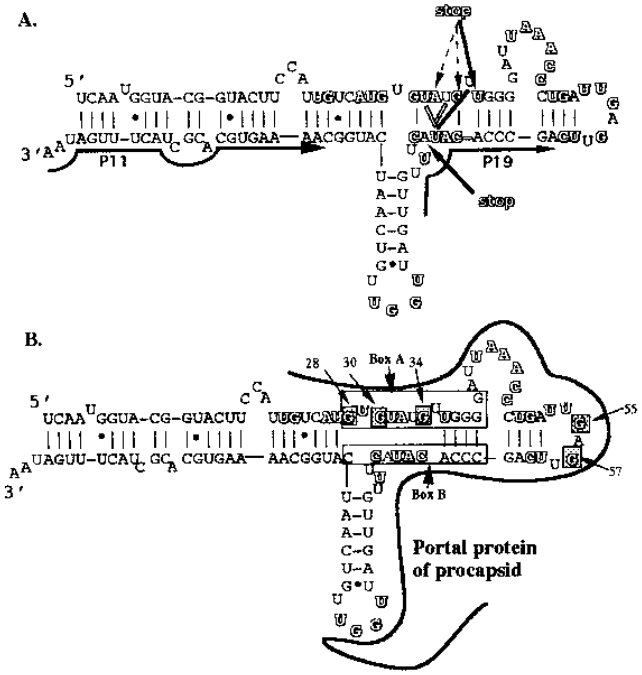

FIG. 5. Schematic diagram showing psoralen cross-linking sites (A) and the region containing bases with varied cleavage patterns (B). P11 and P19 were the two primers used for primer extension. Primer extension stop sites are marked in panel A with solid arrows for strong stops and dashed arrows for weak stops. The cross-linked U pairs are indicated with a solid bar corresponding to a strong stop and open bars corresponding to weak stops. Bases that have been shown to interact directly with procapsids (22) are outlined. In panel B, regions of conformational change detected by RNase T_1 probing are boxed, and guanines that showed different cleavage patterns in the presence and absence of Mg^{2+} are shaded and marked with arrows.

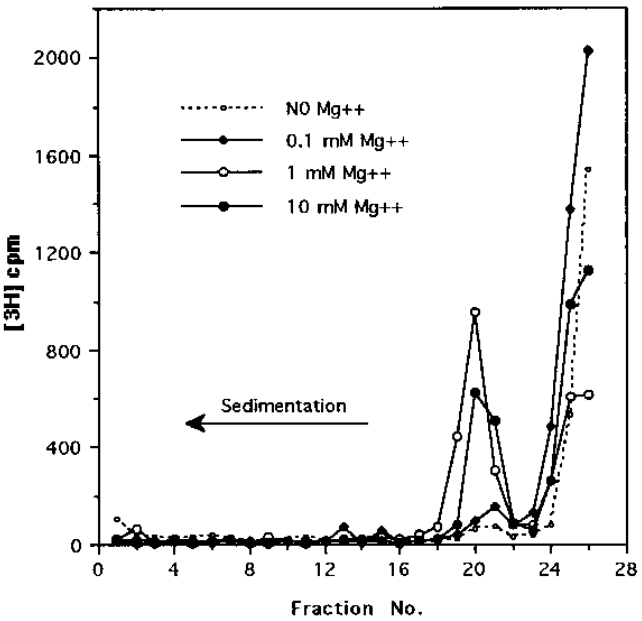

FIG. 6. Determination of minimum Mg^{2+} concentration required for the binding of pRNA to procapsids. [^{3}H]pRNA was incubated with procapsids in the absence or presence of 0.1, 1, and 10 mM Mg^{2+}. The mixture was then subjected to 5 to 20% sucrose gradient sedimentation (from right to left). In the presence of 1 or 10 mM Mg^{2+}, [^{3}H]pRNA bound to procapsids and the complexes were centered at fraction 20. The procapsid-pRNA complex was not detected when the Mg^{2+} concentration was 0.1 mM.

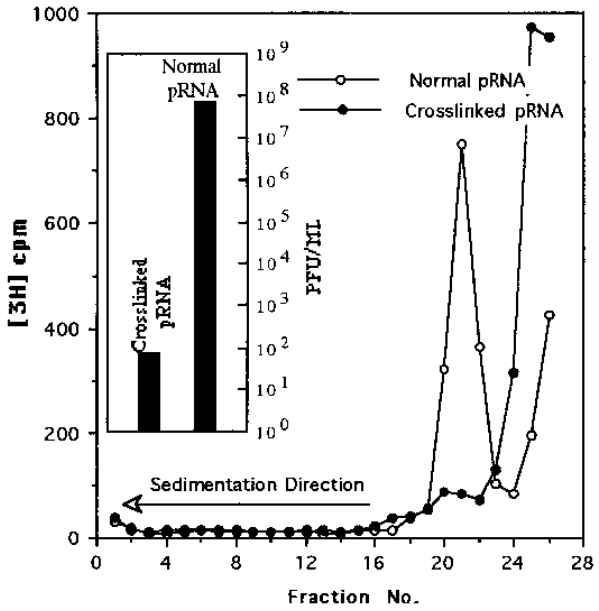

FIG. 7. Assay of activities of normal and cross-linked pRNAs in procapsid binding and DNA packaging (inset).

sence of Mg^{2+}, box A and box B are proximal. In the presence of Mg^{2+}, box A and box B could not be cross-linked by psoralen, suggesting that the interaction of boxes A and B was altered. In addition, primer extension of cross-linked pRNA demonstrated more than one stop. It is possible that more than one pRNA conformation might exist in solution. All stops were located in the region comprising box A and box B. This region has been reported to contact procapsids directly (22). The results of cross-linking suggest that Mg^{2+} induced a transition or refolding of box A and box B that led to the exposure of the procapsid binding sequence. They also imply that such a transition or refolding occurred before pRNA binds to procapsid. This implication was supported by the cleavage pattern of T_1 nuclease and native gel electrophoresis. T_1 RNase digestion and native gel electrophoresis revealed a conformational change of pRNA in the presence of Mg^{2+} without the presence of procapsids. This implication is further supported by the fact that when box A and box B were fastened by cross-linking, thus losing the flexibility to refold, neither procapsid binding capacity nor DNA packaging activity was detected. Although it still cannot be completely ruled out that all the changes reported in this communication were the consequence of Mg^{2+} binding to this region, all evidence reported here supports the conclusion that Mg^{2+} induced a conformational change of pRNA by inducing the shifting or refolding of box A and box B, thus generating a pRNA with a nascent conformation competent to bind procapsids.

ACKNOWLEDGMENTS

We thank Mark Trottier for his comments and Elke Scholz for technical assistance.

This work was supported by NIH grant GM48159.

REFERENCES

1. **Bailey, S., J. Wichitwechkarn, D. Johnson, B. Reilly, D. Anderson, and J. W. Bodley.** 1990. Phylogenetic analysis and secondary structure of the *Bacillus subtilis* bacteriophage RNA required for DNA packaging. J. Biol. Chem. **265:**22365–22370.
2. **Bazinet, C., and J. King.** 1985. The DNA translocation vertex of dsDNA

bacteriophages. Annu. Rev. Microbiol. **39:**109–129.
3. **Bjornsti, M. A., B. E. Reilly, and D. L. Anderson.** 1981. *In vitro* assembly of the *Bacillus subtilis* bacteriophage ϕ29. Proc. Natl. Acad. Sci. USA **78:**5861–5865.
4. **Cimino, G. D., H. B. Gamper, S. T. Isaacs, and J. E. Hearst.** 1985. Psoralens as photoactive probes of nucleic acid structure and function: organic chemistry, photochemistry, and biochemistry. Annu. Rev. Biochem. **54:**1151–1193.
5. **Guo, P., S. Bailey, J. W. Bodley, and D. Anderson.** 1987. Characterization of the small RNA of the bacteriophage ϕ29 DNA packaging machine. Nucleic Acids Res. **15:**7081–7090.
6. **Guo, P., S. Erickson, and D. Anderson.** 1987. A small viral RNA is required for *in vitro* packaging of bacteriophage ϕ29 DNA. Science **236:**690–694.
7. **Guo, P., S. Erickson, W. Xu, N. Olson, T. S. Baker, and D. Anderson.** 1991. Regulation of the phage ϕ29 prohead shape and size by the portal vertex. Virology **183:**366–373.
8. **Guo, P., S. Grimes, and D. Anderson.** 1986. A defined system for *in vitro* packaging of DNA-gp3 of the *Bacillus subtilis* bacteriophage ϕ29. Proc. Natl. Acad. Sci. USA **83:**3505–3509.
9. **Guo, P., C. Peterson, and D. Anderson.** 1987. Prohead and DNA-gp3-dependent ATPase activity of the DNA packaging protein gp16 of bacteriophage ϕ29. J. Mol. Biol. **197:**229–236.
10. **Guo, P., C. Peterson, and D. Anderson.** 1987. Initiation events in *in vitro* packaging of bacteriophage ϕ29 DNA-gp3. J. Mol. Biol. **197:**219–228.
11. **Guo, P., B. Rajogopal, D. Anderson, S. Erickson, and C.-S. Lee.** 1991. sRNA of bacteriophage ϕ29 of *B. subtilis* mediates DNA packaging of ϕ29 proheads assembled in *E. coli*. Virology **185:**395–400.
12. **Guo, P., E. Scholz, J. Turek, R. Nordgren, and B. Maloney.** 1993. Assembly of avian infectious laryngotracheitis virus. Am. J. Vet. Res. **54:**2031–2039.
13. **Harris, M., J. Nolan, A. Malhotra, J. Brown, S. Harvey, and N. Pace.** 1994. Use of photoaffinity crosslinking and molecular modeling to analyze the global architecture of ribonuclease P RNA. EMBO J. **13:**3953–3963.
14. **Hatfield, L., and P. Hearing.** 1993. The NFIII/OCT-1 binding site stimulates adenovirus DNA replication in vivo and is functionally redundant with adjacent sequences. J. Virol. **67:**3931–3939.
15. **Hui, C. F., and C. R. Cantor.** 1985. Mapping the location of psoralen crosslinks on RNA by mung bean nuclease sensitivity of RNA-DNA hybrids. Proc. Natl. Acad. Sci. USA **82:**1381–1385.
16. **Laing, L. G., T. C. Gluick, and D. E. Draper.** 1994. Stabilization of RNA structure by Mg ions: specific and non-specific effects. J. Mol. Biol. **237:**577–587.
17. **Lee, C. S., and P. Guo.** 1994. A highly sensitive system for the assay of *in vitro* viral assembly of bacteriophage ϕ29 of *Bacillus subtilis*. Virology **202:**1039–1042.
18. **Lee, C. S., and P. Guo.** 1995. In vitro assembly of infectious virions of double-stranded DNA phage ϕ29 from cloned gene products and synthetic nucleic acids. J. Virol. **69:**5018–5023.
19. **Lee, C. S., and P. Guo.** 1995. Sequential interactions of structural proteins in phage ϕ29 procapsid assembly. J. Virol. **69:**5024–5032.
20. **Martin, A. C., R. Lopez, and P. Garcia.** 1996. Analysis of the complete nucleotide sequence and functional organization of the genome of *Streptococcus pneumoniae* bacteriophage Cp-1. J. Virol. **70:**3678–3687.
21. **Parsons, B. L., and D. J. Pickup.** 1990. Transcription of orthopoxvirus telomeres at late times during infection. Virology **175:**69–80.
22. **Reid, R. J. D., J. W. Bodley, and D. Anderson.** 1994. Characterization of the prohead-pRNA interaction of bacteriophage ϕ29. J. Biol. Chem. **269:**5157–5162.
23. **Reid, R. J. D., F. Zhang, S. Benson, and D. Anderson.** 1994. Probing the structure of bacteriophage ϕ29 prohead RNA with specific mutations. J. Biol. Chem. **269:**18656–18661.
24. **Trottier, M., and P. Guo.** 1997. Approaches to determine stoichiometry of viral assembly components. J. Virol. **71:**487–494.
25. **Trottier, M., C. L. Zhang, and P. Guo.** 1996. Complete inhibition of virion assembly in vivo with mutant pRNA essential for phage ϕ29 DNA packaging. J. Virol. **70:**55–61.
26. **Turnquist, S., M. Simon, E. Egelman, and D. Anderson.** 1992. Supercoiled DNA wraps around the bacteriophage ϕ29 head-tail connector. Proc. Natl. Acad. Sci. USA **89:**10479–10483.
27. **Wassarman, D. A.** 1993. Psoralen crosslinking of small RNAs *in vitro*. Mol. Biol. Rep. **17:**143–151.
28. **Wichitwechkarn, J., S. Bailey, J. W. Bodley, and D. Anderson.** 1989. Prohead RNA of bacteriophage ϕ29: size, stoichiometry and biological activity. Nucleic Acids Res. **17:**3459–3468.
29. **Wichitwechkarn, J., D. Johnson, and D. Anderson.** 1992. Mutant prohead RNAs in the *in vitro* packaging of bacteriophage ϕ29 DNA-gp3. J. Mol. Biol. **223:**991–998.
30. **Youvan, D. C., and J. E. Hearst.** 1982. Sequencing psoralen photochemically reactive sites in *E. coli* 16s ribosomal RNA. Anal. Biochem. **119:**86–89.
31. **Zacharias, M., and P. J. Hagerman.** 1995. Bulge-induced bends in RNA: quantification by transient electric birefringence. J. Mol. Biol. **247:**486–500.
32. **Zhang, C. L., C.-S. Lee, and P. Guo.** 1994. The proximate 5′ and 3′ ends of the 120-base viral RNA (pRNA) are crucial for the packaging of bacteriophage ϕ29 DNA. Virology **201:**77–85.
33. **Zhang, C. L., K. Garver, and P. Guo.** 1995. Inhibition of phage ϕ29 assembly by antisense oligonucleotides targeting viral pRNA essential for DNA packaging. Virology **211:**568–576.
34. **Zhang, C. L., T. Tellinghuiesn, and P. Guo.** 1995. Confirmation of the helical structure of the 5′/3′ termini of the essential DNA packaging pRNA of phage ϕ29. RNA **1:**1041–1050.
35. **Zhang, C. L., M. Trottier, and P. X. Guo.** 1995. Circularly permuted viral pRNA active and specific in the packaging of bacteriophage ϕ29 DNA. Virology **207:**442–451.